THREE DIMENSIONAL ACQUISITION OF COLORED OBJECTS

N. Schön, P. Gall, G. Häusler

Chair for Optics
Friedrich Alexander University Erlangen-Nuremberg
Staudtstr. 7 / B2, 91058 Erlangen, Germany
e-mail: kschoen@optik.physik.uni-erlangen.de
URL: www.optik.uni-erlangen.de/osmin

Abstract

In this paper we present a system for the acquisition of color and shape of free form surfaces. We place the emphasis on the methods for the acquisition and reconstruction of surface color. We discuss algorithms to eliminate illumination effects such as shading and specular highlights. We will further describe a procedure to merge the color information of multiple range images, utilising redundancy in overlapping regions, thus enhancing the appearance of the object.

1 INTRODUCTION

Our research of optical 3d sensors has led to a standard method for the complete digitization of free form surfaces, including their color texture. The method is a processing pipeline consisting of several steps:

1. **Data acquisition:** We use an optical 3d sensor based on the principle of phase-measuring triangulation [1]. Multiple range and (pixel identical) color images of the object are taken to acquire the whole object surface.
2. **Surface registration:** The range images are transformed into a common coordinate system. First, they are interactively and coarsely registered to each other. Then, an ICP algorithm automatically minimizes the deviations between overlapping range images.
3. **Mesh reconstruction and data modeling:** The geometry data of the different views are merged into one single topological structure, a triangle mesh. A smoothing algorithm reduces noise, using redundant information in overlapping regions. A curvature dependent mesh thinning is applied, to get a more compact surface representation.
   Steps 1. – 3. are illustrated in Fig. 3.
4. **Color reconstruction:** For each range image, a corrected color image is created from the original color images by removing effects that depend only on the illumination of the acquisition scene. The color images are merged to get a texture representation for the complete triangle mesh obtained from step 3.

Other researchers have already proposed similar systems. Baribeau et al. [2] use a chromatic laser range sensor to acquire geometry data. Sato and Ikeuchi use a standard fringe projection method and simplify the registration by using a turn table with known rotation angles [3].
Both separate object color from illumination effects by geometrical analysis in color space and subtraction of the specular component from the color signal.
In this paper we concentrate on the objectives “data acquisition”, as far as color data are concerned, and “color reconstruction”.
For the topic “surface registration” refer to [4]. “Mesh reconstruction” and “data modeling” are discussed in detail in [5].

2 DATA ACQUISITION

Data acquisition is performed in two steps: Acquisition of 3d data and acquisition of color data.
The 3d sensor is based on the principle of phase measuring triangulation. A binary mask is used to generate very accurate sinusoidal fringes by astigmatic projection [6]. The mask is realized by a ferro-electric crystal modulator (FLC) to perform a fast phase shift. A sequence of eight different fringe patterns is acquired for one 3d-measurement. Because of the short switching times of ferro-electric crystals a complete 3d range image can be measured in 320 ms, using a standard CCD camera [7]. The sensor can be easily scaled for a measuring field of 5x5x5 mm^3 up to 1x1x1 m^3. A measuring uncertainty of about 1:2000 of the longitudinal measuring range is achieved. The geometry data sets consist of coordinate triples *(x,y,z)* arranged in a matrix, as on the CCD chip of the camera.
To enable capturing of color images, instead of a B/W camera, we now use a 3-chip color-CCD-camera.
After the measurement of each range image, two color images without fringes are taken, with different directions of illumination. The angle between the illumination directions has to be large enough that the inevitable specular highlights appear in non-overlapping regions. This is a precondition for the elimination of specular reflection. We use halogen lamps with a small diameter (< 5 cm with a distance of approx. 2 m from the object), so that we can mathematically model them as point light sources.
The main advantage of using the same camera for geometry and color measurement is, that geometry and color data that correspond to the same surface point have identical row and column indices in the captured images.

3 ELIMINATION OF ILLUMINATION EFFECTS

A color video image of an object does not show the true color of the object's surface, but it contains effects that are caused by the illumination conditions during acquisition. We adress here the effects of shading and specular highlights. Shading means the local variations of reflected radiance dependent on the surface inclination against the illumination direction. Specular highlights appear for parts of the surface, where the direct reflection of the incident light is visible for the camera. To eliminate these effects, three processing steps are performed, separately for each color channel:

1) The local influence of direction and distance of illumination is compensated in the color images.
2) For each color image, a "confidence mask" is created. This structure assigns to each color pixel a value, that represents a measure of its quality. It depends on the influence of noise and specular reflection on the corrected color.
3) For each range image a final color image is created. The two corrected color images are superimposed using the values of the confidence mask as interpolation weights.

In contrast to other researchers, who subtract the specular highlights from the original color data, our approach segments specular highlights in the color images and replaces them by undistorted data. This has the advantage, that the dynamics of the camera doesn't have to be adjusted to the intensity of the highlights, so we make better use of the dynamical range of the camera.

Reflection Model

In order to compensate for illumination effects, we will describe the reflection of light by the BRDF (Bidirectional Reflection Distribution Function) $f_r(\theta_1,\varphi_1,\theta_2,\varphi_2)$ [8]. For a specific point on the surface, it is defined as

$$f_r(\theta_1,\varphi_1,\theta_2,\varphi_2) := \frac{dL_2(\theta_2,\varphi_2)}{dL_1(\theta_1,\varphi_1)} \qquad (1)$$

where $L_1(\theta_1,\varphi_1)$ ist the incident radiance arriving from illumination direction (θ_1,φ_1) and $L_2(\theta_2,\varphi_2)$ is the reflected radiance in observation direction (θ_2,φ_2) (see Fig. 1).

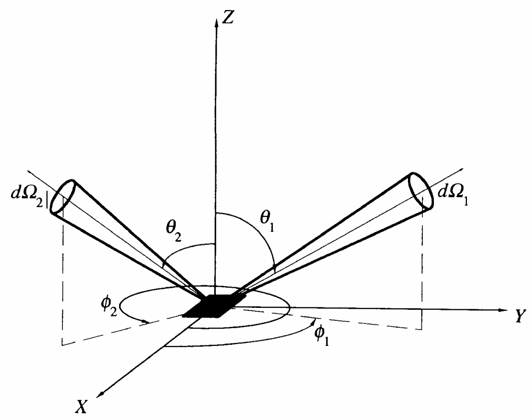

Fig. 1: Geometry of BRDF model for light reflection. Z-direction coincides with surface normal.

We further assume, that the reflection can be divided into two components, the diffusely reflected component L_D and the specular reflected component L_S:

$$L_2 = L_D + L_S \qquad (2)$$

The diffusely reflected component is approximated by Lambertian reflection,

$$dL_D(\theta_1, r) = f_{rD} \cdot dE = f_{rD} \cdot \frac{dI\cos(\theta_1)}{4\pi r^2}, \quad -\tfrac{\pi}{2} \le \theta_1 \le \tfrac{\pi}{2}, \qquad (3)$$

with the irradiance *E* arriving at the surface, the Intensity *I* of the light source illuminating the scene and the distance *r* between surface point and light source. The *cos*-term reflects the “shading”, i.e. the dependency between surface radiance and its inclination against the illumination direction (see Fig. 4).

The specularly reflected component is described by a Gaussian distribution of radiance around the “mirror direction”, i.e. the direction into which a mirror with the same surface normal as the considered point would reflect the incoming light:

$$dL_S(\theta_1,\varphi_1,\theta_2,\varphi_2,r) = f_{rS}(\theta_1,\varphi_1,\theta_2,\varphi_2)\frac{dI\cos(\theta_1)}{4\pi r^2} \qquad (4)$$

$$f_{rS}(\theta_g) = \frac{1}{\sqrt{2\pi}\sigma_S\cos(\theta_1)} \cdot \exp\left(-\frac{\theta_g{}^2}{2\sigma_S{}^2}\right) \qquad (5)$$

Here, σ_s is the angular width of the specular highlights and depends on the roughness of the surface. θ_g is the angle between the “mirror normal” and the normal of the current surface point. The mirror normal is the direction that the surface normal would have for direct reflection of the incident ray into the viewing direction of the camera.

f_{rD} and σ_s are the illumination independent properties, that we estimate for making an object-centered description of surface reflection are the parameters. f_{rD} depends on the location, but is independent from illumination and viewing direction. Thus it represents the texture of the surface. Actually, each color channel of each pixel has a different f_{rD}, depending on the color of the surface. σ_s expresses the so called “shininess” of the surface.

Compensation of the direction and distance of illumination

We can regard the pixels of the color image as measurements of $L_2(\theta_v, \varphi_v)$, up to a constant factor, with (θ_v, φ_v) being the viewing direction of the camera. We will ignore the constant, because in any case the results will be normalized.
Since the coordinates of each surface point and the position of the point light source are known, we can compute θ_1 and *r* for each surface point. Multiplication of the color pixel intensities by $c_{corr} = \dfrac{r^2}{\cos(\theta_1)}$ eliminates the influence of the distance from and the inclination against the light source (see Eqs. (3) and (4)). The result are two corrected color images. They still include, however, distortions caused by noise and specular reflection.

Estimation of the influence of noise and specular highlights

The influence of noise and specular highlights on the corrected color pixels is represented by confidence values. They correspond to a posteriori probabilities for the truth of certain hypotheses concerning the result of a measuring or processing step.
The noise depends primarily on two quantities:

1) The intensity m_0 of the pixel in the original color image,
2) the factor c_{corr} that was used to correct the color value.

The confidence value $k_a(m_0)$ for the original intensities corresponds to the probability, that the true original intensity m_0 lies in the interval $[m_0 - \Delta m_0, m_0 + \Delta m_0]$, where Δm_0 is defined by the expression

$$\Delta m_0 = \sigma \cdot \frac{m_0}{m_{\max}} \qquad (6)$$

with the standard deviation σ of the original intensities and the maximum of all original intensities $m_{\max}$. $k_a(m_0)$ increases with increasing intensity.
The confidence value $k_b(c_{corr})$ for the correction factor c_{corr} corresponds to the probability, that the true corrected color value m lies in the interval $[m - \Delta m, m + \Delta m]$, where Δm is constant for all m and is chosen to adapt the noise on the 3d geometry data. $k_b(c_{corr})$ decreases with increasing c_{corr}.
The quantitative description of the influence of specular reflection by confidence values is somewhat more complicated. We first have to determine the angular width of the highlights observed on the surface, before we can use Eqs. (4) and (5) to compute the specularity of each pixel.
To measure the angular width σ_s of specular highlights, they have to be segmented in the color images. We use a segmentation based on the the fact, that glossy regions constitute the brightest areas in the image. First, the brightest spots in the image are taken as seed points for a region growth algorithm. The region around these pixels is grown until pixels are reached, where the intensity lies under a certain threshold (see Figs. 5 and 6).
We compute θ_g, the angular deviation between local surface normal and the mirror normal, for each border point of such a region. The final σ_s is the average from all segmented glossy regions.
According to the applied reflection model, the probability that a pixel is affected by specular reflection is given by

$$k_{spec}(\theta_g) = 1 - \exp\left(-\frac{{\theta_g}^2}{2{\sigma_s}^2}\right) \qquad (7)$$

For pixels that don't show any influence of specular highlights, we have $L_S \approx 0$. Then the confidence value for specularity is maximum, i.e. $k_{spec} \approx 1$ (see Fig. 2).

Fig. 2: Examples of confidence masks for influence of specular reflection. Left: illumination from left. Right: Illumination from right. Note that the highlights (black regions, i.e. low confidence values) are in non-overlapping areas.

The final confidence value $k(m_0, c_{corr}, \theta_g)$, combining the quality measures for noise *and* specular reflection, is then

$$k(m_0, c_{corr}, \theta_g) = k_a(m_0) k_b(c_{corr}) k_{spec}(\theta_g) \quad (8)$$

Superimposing the color images

The final color image is created from the two corrected color images by weighted interpolation of the color values of the pixels. The interpolation weights are computed from the confidence values already discussed. The resulting value of the red component $\hat{R}$ of a pixel is obtained from

$$\hat{R} = \frac{k_{left} R_{left} + k_{right} R_{right}}{k_{left} + k_{right}} \quad (9)$$

with the final confidence values for the color images with illumination from left (k_{left}) and right (k_{right}) and the values of their corrected red color channels, R_{left} and R_{right}. Analogous equations hold for the blue and green channel.

Now we have for each range image a map with the "pure" color of each surface sample point, called "texture map". This structure, however, doesn't reflect the topological mesh representation, into which the geometry data are transformed by the processing pipeline.

4 MERGING MULTIPLE VIEWS

If merging of the texture maps of multiple views is done by simply filling the triangles of the thinned mesh with the corrected texture from different views and joining them according to their topology, steps in intensity arise between textures from different views. The reason for this is primarily, that the applied illumination model is not accurate enough. To avoid those artifacts, texture merging has to be performed in several steps:

1. The correspondences between points of all range images are established. For each sample point $\vec{x}_a$, the closest sample points $\vec{x}_{b,i}$ in all overlapping views are determined, using a kd-tree structure for efficient search. Then, the corresponding surface points

$\vec{x}'_{a,i}$ are interpolated in the adjacency of the closest sample point. To increase accuracy, the interpolation uses the position of the measuring camera of the considered range image. A viewing ray is traced from the camera position through the considered sample point $\vec{x}_a$. The intersections of the ray with the surfaces of the overlapping views are the interpolated points $\vec{x}'_{a,i}$.

2. The color data of all corresponding surface points are interpolated. The interpolation weights are additional confidence values. They reflect the fact, that the quality of the texture data is high for points, where the normal direction is near to the viewing direction. This step results in new texture maps, which contain color values, that are adapted between the views and reduce intensity steps between them.
3. For each triangle of the final mesh of the complete object, the "best" texture triangle is chosen from all range texture maps. A closest point search is done for the corner points of the triangle to find all corresponding point-triples in the range images. Via their row and column values, they give a direct link to the corresponding positions in the texture map. Their confidence values are used as criteria for the optimal choice of the texture map, from which the triangle texture will be taken. References to the corners of the texture triangle (called "texture coordinates") are stored with the vertices of the triangle in the mesh.

The representation of a textured object via texture maps and a triangle mesh with texture coordinates is a data structure suitable for standard rendering hardware. This enables the fast and realistic visualization of digitized colored 3d objects (see Fig. 7).

References

[1] M. Halioua, H. Liu, V. Srinivasan: Automated phase-measuring profilometry of 3-D diffuse objects. *Appl. Opt.* **23**, (1984) 3105 – 3108.

[2] Baribeau, R., Rioux, M., Godin, G., "Color reflectance modeling using a polychromatic laser range sensor", *IEEE Trans. Pattern Analysis and Machine Intelligence*, Vol. 14, No. 2, pp. 263-269, (1992).

[3] Sato, Y., Ikeuchi, K., „Reflectance Analysis for CG Model Generation"*, Graphical Models and Image Processing*, Vol. 58, No. 5, September (1996).

[4] G. Häusler u. D. Ritter. „Matching and Registration of 3D-Surfaces Measured with Optical 3D-Sensors in Unknown Positions", *IEEE Transactions on Pattern Analysis and Machine Intelligence* (1997).

[5] St. Karbacher, X. Laboureux, N. Schön und G. Häusler. „Processing Range Data for Reverse Engineering and Virtual Reality.", In *Proceedings of Third International Conference on 3-D Digital Imaging and Modeling* (2001), Quebec, Canada, 314-321, IEEE 2001

[6] M. Gruber u. G. Häusler. "Simple, robust and accurate phase-measuring triangulation" *Optik 89*, No. 3 (1992) 118-122

[7] G. Bohn, L. Cloutot, H.-P. Habermeier, R. Lampalzer, A. Schröter, N. Schön, K. Veit und G. Häusler. „Fast 3d – Camera for Industrial and Medical Applications". *Proc. of ODIMAP II*, 214-219, 2nd Topical Meeting on Optoelectronic Distance/Displacement, Measurements and Applications, University of Pavia, Italy, May 20-22, 1999.

[8] Nicodemus, F. E., Richmond, J. C., Hsia, J. J., Ginsberg, I. W., Limperis, T.: *Geometrical Considerations and Nomenclature for Reflectance (Monograph 160).* U.S. Department of Commerce, National Bureau of Standards, Washington (1977).

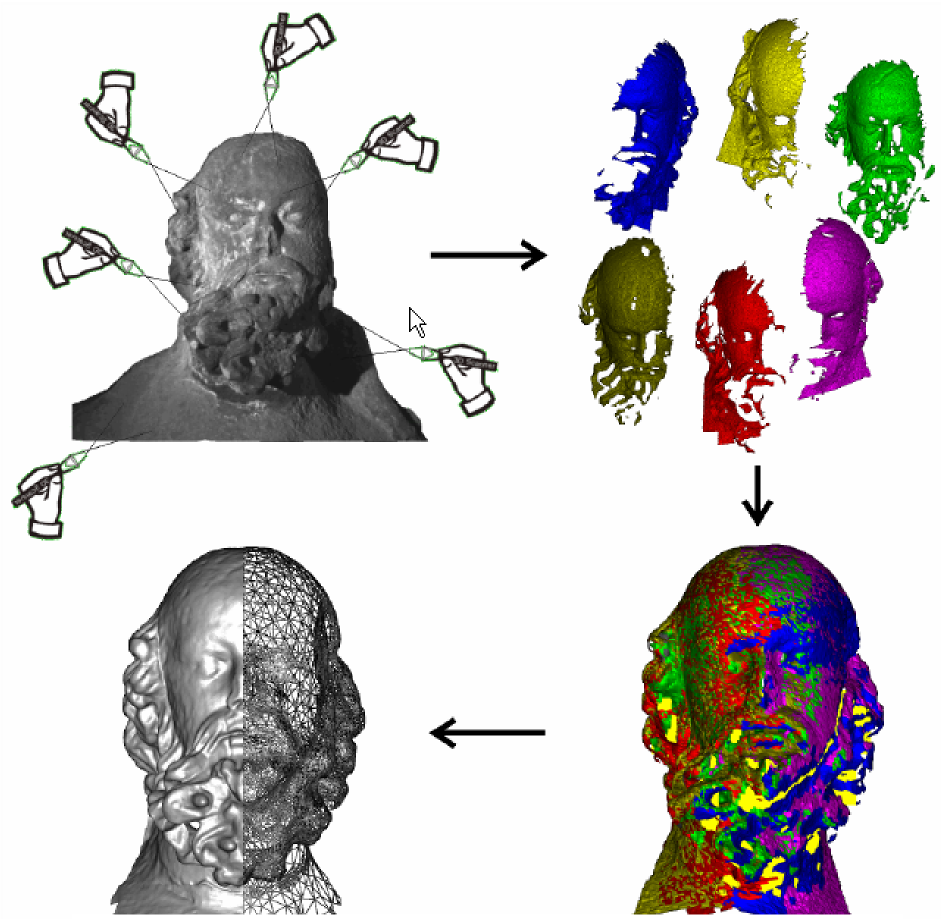

Fig. 3: Data acquisition (upper left), registration (right) and mesh reconstruction (lower left) of the head of an antique statue.

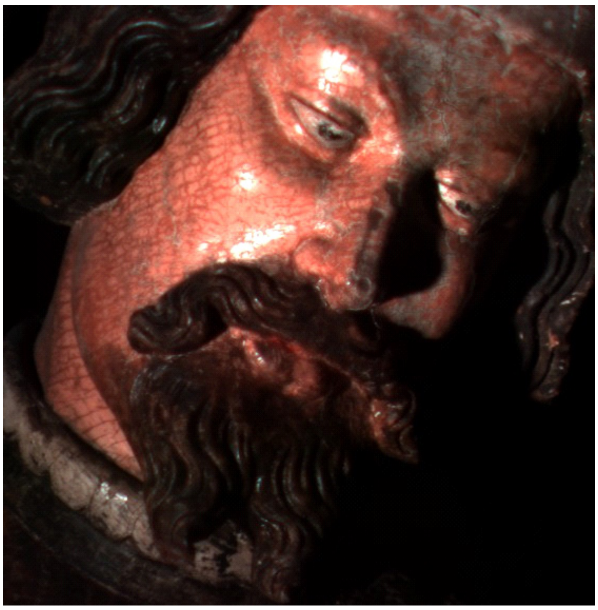

Fig. 4: One of the two color images taken in addition to the 3d range image.
Specular highlights and shading are visible.

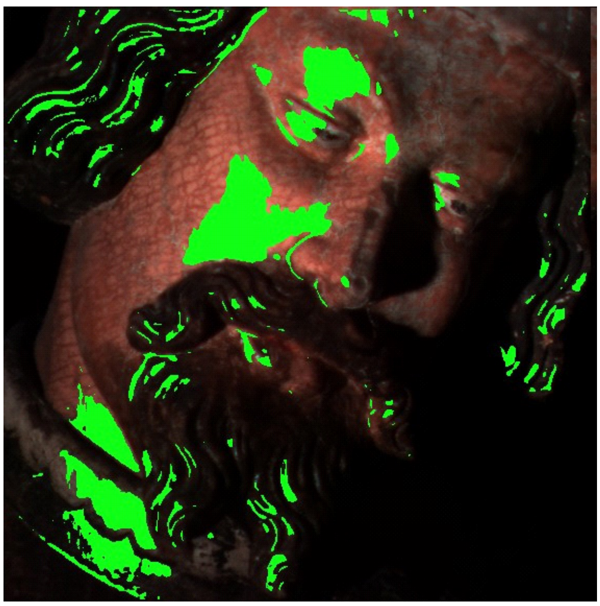

Fig. 5: Segmentation of specular highlights by a region growth algorithm.

Fig. 6: Visualization of a St. George statue from the Germanic National Museum, Nuremberg.
Left: Only geometry, without texture. Right: With reconstructed texture.